CONF-961017--7
ANL/ES/CP--90529

STUDY OF USING OXYGEN-ENRICHED COMBUSTION AIR FOR LOCOMOTIVE DIESEL ENGINES

Ramesh B. Poola and Raj Sekar
Argonne National Laboratory
Argonne, Illinois

Dennis N. Assanis
The University of Michigan
Ann Arbor, Michigan

G. Richard Cataldi
Association of American Railroads
Washington, D.C.

ABSTRACT

A thermodynamic simulation is used to study the effects of oxygen-enriched intake air on the performance and nitrogen oxide (NO) emissions of a locomotive diesel engine. The parasitic power of the air separation membrane required to supply the oxygen-enriched air is also estimated. For a given constraint on peak cylinder pressure, the gross and net power output of an engine operating under different levels of oxygen enrichment are compared with those obtained when a high-boost turbocharged engine is used. A 4% increase in peak cylinder pressure can result in an increase in net engine power of approximately 13% when intake air with an oxygen content of 28% by volume is used and fuel injection timing is retarded by 4 degrees. When the engine is turbocharged to a higher inlet boost, the same increase in peak cylinder pressure can result an improvement in power of only 4%. If part of the significantly higher exhaust enthalpies available as a result of oxygen enrichment are recovered, the power requirements of the air separator membrane can be met, resulting in substantial net power improvements. Oxygen enrichment with its attendant higher combustion temperatures, reduces emissions of particulates and visible smoke but increases NO emissions (by up to three times at 26% oxygen content). Therefore, exhaust gas after-treatment and heat recovery would be required if the full potential of oxygen enrichment for improving the performance of locomotive diesel engines is to be realized.

INTRODUCTION

Both railroads and engine manufacturers face a major challenge if they are to meet the standards for emissions of smoke, particulates, unburned hydrocarbons, and oxides of nitrogen (NO_x) set forth in the U.S. Environmental Protection Agency's proposed regulations for locomotive diesel engines. Railroads also face an increasing demand for higher motive power so payloads in freight locomotives can be increased. Argonne National Laboratory and the Association of American Railroads initiated a cooperative research and development agreement to study the application of oxygen-enriched intake air as one method to meet the above challenges.

A number of analytical and experimental studies (e.g., Sekar et al., 1990; Sekar et al., 1991a&b; Marr et al., 1993) have demonstrated the benefits of using oxygen-enriched intake air in diesel engines. Increasing the oxygen content of a reacting fuel-oxidizer mixture leads to faster burn rates and the ability to burn more fuel at the same stoichiometry (oxygen-to-fuel ratio). These effects have the potential to increase the thermal efficiency and specific power output of a diesel engine. The power increase from a given displacement engine can be suitably exploited to increase the number of locomotive cars or freight. In addition, oxygen enrichment can also be considered as a way to reduce the sudden loss in power output when locomotives operate in underground tunnels and at high altitudes.

When oxygen is added to the combustion air, emissions of visible smoke, particulates, and unburned hydrocarbons decrease significantly over a wide-load range as a result of the more complete combustion (e.g., Iida and Sato, 1988). Added oxygen also leads to shorter ignition delays and offers the potential for burning lower grade and nonpetroleum fuels (Iida and Sato, 1988; Sekar, et al., 1990). However, the increased oxygen content in the combustion air is also expected to increase NO_x emission levels because of the higher combustion temperatures. The anticipated increase in NO_x emissions could be controlled by retarding fuel injection timing and by using other state-of-the-art concepts such as exhaust post-treatment with monatomic nitrogen and lean-NO_x catalysts. The objective of the work discussed here was to address, in a systematic way, the key technical issues associated with applying oxygen-enrichment technology to locomotive diesel engines. These issues include (1) optimizing the level of oxygen enrichment in the intake air (2) designing an air

DISCLAIMER

separation membrane and assessing its parasitic power requirements and (3) exploring the merits of injection retard for controlling peak pressure and NO emissions.

In the present work, an appropriately modified computer simulation of a turbocharged diesel engine was used to study the effects of oxygen-enriched intake air on the performance and NO emissions of a locomotive diesel engine. The physical and operating characteristics of an air separation membrane were briefly reviewed, and a simplified model was proposed to estimate the module size and parasitic power required to supply the desired oxygen-enrichment level in the intake air. On the basis of engine and membrane models, the net improvements in brake power achieved by an engine equipped with an air separation membrane to supply the oxygen-enriched intake air were computed. Use of oxygen-enriched air was compared with turbocharging to a higher inlet boost as a means to increase power output. The effects of retarded fuel injection timing were also studied in conjunction with oxygen-enriched intake air. Finally, the potential for enhanced exhaust heat recovery when using oxygen enrichment was assessed. Other aspects of oxygen enrichment, such as a reduction in particulates, smoke, and unburned hydrocarbons and the ability to burn lower grade fuels, are not the subject of this paper but have been studied earlier (e.g., Sekar et al., 1990; Sekar et al., 1991a&b).

SUMMARY OF DIESEL ENGINE SIMULATION

The model used for this study is based on a zero-dimensional, thermodynamic simulation of a turbocharged diesel engine (Assanis and Heywood, 1986). The parent code was validated against test results from a Cummins engine (Assanis and Heywood, 1986) and modified to allow for various levels of oxygen enrichment in the intake air and for operation with water-emulsified fuels (Assanis et al., 1990). This section briefly summarizes the main assumptions of the simulation. Additional details on the parent code can be found in Assanis and Heywood (1986).

The diesel four-stroke cycle is treated as a sequence of continuous processes: intake, compression, combustion (including expansion), and exhaust. Quasi-steady, adiabatic, one-dimensional flow equations are used to predict mass flows past the intake and exhaust valves. The compression process is defined to include the ignition delay period (i.e., the time interval between the start of the injection process and the ignition point). The total length of the ignition delay can be either specified or predicted by using an Arrhenius expression that is based on the mean cylinder gas temperature and pressure during the delay period. Combustion is modeled as a uniformly distributed heat release process. The rate of heat release is specified by using an algebraic burning rate correlation. Heat transfer is included in all the engine processes. Convective heat transfer is modeled by using available engine correlations that are based on turbulent flow in pipes. The characteristic velocity and length scales required to evaluate these correlations are obtained from a mean and turbulent kinetic energy model. Radiative heat transfer, based on the predicted flame temperature, is added during combustion. For this work, a heat release correlation that was developed earlier and was based on experimental data for oxygen-enriched diesel combustion (Assanis et al., 1993) was used, i.e.,

$$\frac{\dot{m}_{f,b}(\theta)}{m_{f,0}} = \theta^{B_p} \cdot \exp(A_p - C_p \cdot \sqrt{\theta}) + \theta^{B_d} \cdot \exp(A_d - C_d \cdot \sqrt{\theta}) \quad (1)$$

where $\dot{m}_{f,b}$ is the instantaneous rate of fuel burning; $m_{f,o}$ is the total mass of fuel injected; θ is the crank angle after ignition; A, B, C and D are adjustable parameters; and subscripts p and d correspond to the premixed and diffusion combustion phases, respectively. The adjustable parameters are determined by matching the experimental heat release rates against curve-fitted profiles generated by using the above heat release correlation (Equation 1). On the basis of measured heat release data of a single-cylinder diesel engine (Assanis et al., 1993) operating with an oxygen content in the range of 21% to 35% by volume and an overall equivalence ratio of about 0.5, the following values are recommended for the constants

$$\begin{aligned} A_p &= 16.81 - 0.61539\ \%\ O_2 \\ B_p &= 26.625 - 0.70921\ \%\ O_2 \\ C_p &= 28.152 - 0.76602\ \%\ O_2 \\ A_d &= -6.0295 - 0.1692\ \%\ O_2 \\ B_d &= 3.4698 + 0.10564\ \%\ O_2 \\ C_d &= 1.8202 + 0.03195\ \%\ O_2 \end{aligned} \quad (2)$$

The formation and destruction of thermal NO from atmospheric nitrogen have been studied widely on the basis of the extended Zel'dovich mechanism (Lavoie et al., 1970), i.e.,

$$\begin{aligned} O + N_2 &= NO + N \\ N + O_2 &= NO + O \\ N + OH &= NO + H \end{aligned} \quad (3)$$

For the purpose of implementing the NO kinetics model in the diesel simulation, the combustion chamber is divided in two zones: a burned zone containing products of combustion and an unburned zone containing air and residual gas. At any instant throughout combustion, an incremental flux of fuel given by Equation 1 that is accompanied by a stoichiometric flux of air is assumed to cross from the unburned zone to the burned zone. The products of combustion are assumed to be at the adiabatic flame temperature, resulting from combustion of a stoichiometric fuel-air mixture of specified oxygen content at the instantaneous unburned gas temperature and pressure (uniform within the combustion chamber). The kinetic rate of change of the concentration of NO in the postflame gases, along with appropriate expressions for its temperature-dependent rate constants, are obtained from Lavoie et al. (1970). The instantaneous concentrations of NO, O, O_2, OH, H, and N_2 are approximated by their equilibrium values at the specified burned zone temperature and pressure. On the basis of a knowledge of the instantaneous concentration of NO in the burned zone, its overall concentration in the cylinder can be computed by multiplying the ratio of moles in the stoichiometric burned core times the total number of moles in the cylinder.

AIR SEPARATION MEMBRANE

Operating Principle and Modes

Air delivered to engines can be oxygen-enriched in by selective permeation through nonporous, polymer membranes via a well-known "solution-diffusion" mechanism. In this mechanism, air molecules dissolve into the membrane and then diffuse across it. A typical membrane process for air separation is shown in Figure 1. The air is fed to the membrane device at an elevated pressure, where it passes across one side of the membrane. The opposite side of the membrane is held at a low pressure. The pressure differential across the membrane provides the driving force for the diffusion of oxygen and nitrogen across the membrane. Oxygen can diffuse more rapidly and become enriched in the low-pressure permeate stream, while nitrogen is concentrated in the retentate stream.

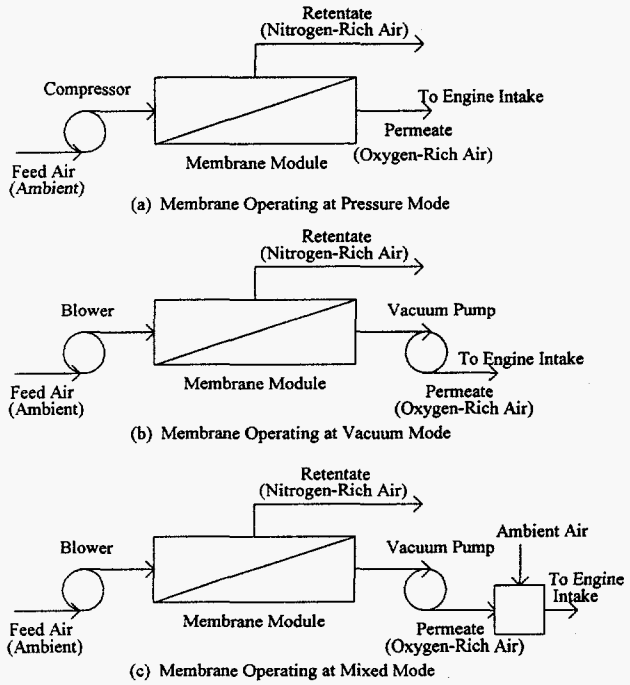

Fig. 1: Air separation membrane modes of operation

Air separation membrane units can be operated in one of three modes as illustrated in Figure 1: vacuum, pressure, or mixed. In the vacuum mode, the feed air is pressurized to only slightly above atmospheric pressure (about 1 to 3 psig), and a vacuum is maintained on the permeate side of the membrane. The retentate is vented at atmospheric pressure. The vacuum mode is typically more energy-efficient than the pressure mode, primarily because a vacuum is applied only on the permeate (product stream). However, because of the limited differential pressure, the vacuum mode requires a larger membrane area for a given flow rate than does the pressure mode. In the pressure mode, the feed air is typically pressurized (by an air compressor) to several atmospheres, while the permeate is maintained at about atmospheric pressure. Higher driving forces are obtained in this mode because the differential pressures are higher than those of the vacuum mode, resulting in reduced membrane area requirements. However, the pressure mode is more energy intensive, because both permeate and retentate have to be compressed to higher pressures. Finally, in the mixed mode, the feed air is pressurized, and a partial vacuum is maintained on the permeate side to increase both the compression ratio and differential pressure and thus the oxygen concentration. The oxygen-enriched air stream from the permeate is then mixed with an ambient air stream to obtain the desired air flow and oxygen concentration. Figure 2 illustrates how a separation membrane operating in the mixed mode would be retrofitted on a turbocharged, multicylinder, diesel engine to enrich the oxygen content of the air delivered to its turbocharger compressor.

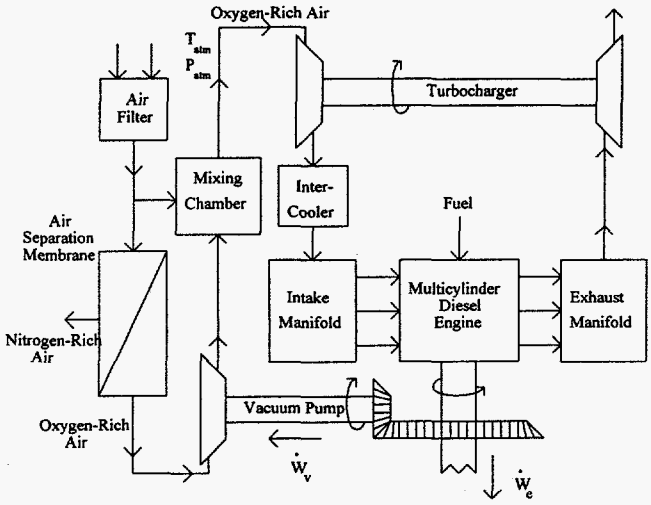

Fig. 2 Turbocharged diesel system configuration using oxygen-rich air supplied by air separation membrane

Membrane Performance and Design

The performance of a membrane is characterized by its permeability and selectivity (intrinsic properties) and stage cut (or recovery). The overall permeability is a function of flow as well as of membrane composition. It can be described by Fick's law as follows (Gollan and Kleper, 1985; Ragland and Whipple, 1989):

$$N_i = \frac{P_{ri} A \Delta P}{\delta} \qquad (4)$$

where N_i is the flow rate of gas i (cm^3 of STP/s); P_r: is the intrinsic permeability of gas i in the membrane (cm^3 of STP - cm/cm^2-s-cm of Hg); A is membrane area (cm^2); δ is the membrane separating barrier thickness (cm); and ΔP is the trans-membrane partial pressure difference of gas i (cm of Hg).

Equation 4 indicates that the degree of separation between the gases clearly depends on the relative permeabilities of the gases to be separated. This ratio of gas permeabilities is known as selectivity or separation factor. The separation factor (α) between oxygen and nitrogen can be calculated as follows:

$$\alpha = \frac{P_{rO}}{P_{rN}} \quad (5)$$

The larger the value of the separation factor is, the better is the separation. The stage cut (φ or recovery) of an air separator is another important measure of performance. It is simply the permeate flow divided by the feed flow rate.

The performance of an air separator depends on several other parameters such as membrane polymer structure, skin thickness, geometry of the fibers, fiber dimensions, flow pattern, feed direction, feed conditions, cartridge type, packaging density, and arrangement of separators. Details are provided in Winston Ho and Sirkar (1992) and Koros and Chern (1987). The selection of a membrane to achieve the desired oxygen-enriched air flow is evaluated in terms of the power required to maintain the differential pressure across the membrane and the amount of space it occupies.

Various mathematical models and calculation methods for designing hollow-fiber membranes have been reported in the literature (Pan, 1986; Chern et al., 1985). The development of a model to study all the performance variables and their tradeoffs would be quite exhaustive and beyond the scope of this paper. In the present work, a Du Pont proprietary code was made available to establish a relationship between the permeate oxygen concentration and stage cut under the specified input conditions listed in Table 1 and at several pressure ratios between the feed and permeate (ranging from 1.5 to 4) in the following form:

$$\%O_2 = A\varphi^3 + B\varphi^2 + C\varphi + D \quad (6)$$

where % O_2 is the permeate oxygen concentration; A, B, C, and D are third-order polynomial coefficients as a function of the pressure ratio between the feed and permeate; and φ is the stage cut. Equation 6 was used to compute the stage cut at several desired permeate oxygen concentrations. Perfluoro-2-2-dimethyl-1-3 dioxole copolymerized with tetrafluoroethylene, being developed at Compact Membrane Systems, Inc. (CMS), is being considered as a membrane material (Nemser and Roman, 1991) in the present model. From the stage cut, feed flow rates corresponding to the permeate flow rate and oxygen concentration can be computed. The pumping work can be computed from the pressure ratio between the feed and permeate and from the feed and permeate flow rates.

In the absence of certain key design data, including the mean partial pressure of oxygen in the module and the fiber geometry, it is difficult to estimate membrane size. However, an attempt was made to demonstrate the influence of membrane properties and other design variables on the membrane's size and power requirements. For comparison purposes, a pressure ratio of 3.0 between the feed and permeate across the membrane was assumed, and the mixed mode was considered as a mode of operation (the mixing stream's concentration was 28% by volume and its flow was about 72% of the total engine air flow). The module size also varies with the active length of the fibers, which is, in turn, a function of pressure drop across the fiber tubes. For purposes of this study, the active length was arbitrarily selected to be 3 or 4 ft. Finally, to calculate the membrane surface area by using Equation 4, the end pressures of oxygen across the feed and permeate were employed instead of the mean partial pressure of oxygen. Membrane volume and module size were computed on the basis of fiber geometry and packing density.

Table 1. Membrane properties and input parameters for two CMS materials

Properties	CMS-3	CMS-7
Permeability (cm^3 of STP-cm/cm^2-s-cm of Hg x 10^{10})		
Oxygen	340	990
Nitrogen	130	480
Selectivity (O_2/N_2)	2.71	2.05
Membrane skin thickness (m)	0.1	0.1
Hollow fiber dimensions (OD/ID), m	660/500	660/500
Packing density	0.5	0.5

RESULTS AND DISCUSSION

Engine Configuration

To explore the effect of various oxygen-enrichment levels in the intake air on engine performance and emissions, a representative 12-cylinder, GE 12-7FDL locomotive diesel engine was selected, and the diesel engine simulation was applied to model its performance. The specifications of the engine geometry are given in Table 2. Locomotive diesel engines are operated at a series of fixed settings (throttle notches 1 through 8), with each one providing a constant amount of power at a governed engine speed. Since turbomachinery maps were not available, the intake and exhaust manifolds were treated as constant pressure and temperature plenums. The intake plenum conditions were specified; the exhaust plenum conditions were predicted by means of ideal thermodynamic models of the compressor and turbine with specified efficiencies. The actual intake and exhaust valve events and the manifold control volumes and surface areas were obtained from a previous study conducted at the Southwest Research Institute (Markworth et al., 1993).

Table 2. Specifications for GE locomotive diesel engine

Bore (mm)	228.6
Stroke (mm)	266.7
Connecting rod length (mm)	589.7
Compression ratio	12.7:1
Displacement volume (L)	10.9
Number of cylinders	12
Number of valves	48
Rated speed (rpm)	1,050
Rated power (bhp)	2,500
Standard injection timing (bTDC)	24

Model Calibration and Validation

The diesel engine model was calibrated through minor tuning of its adjustable constants to correspond with the computation of the discharge and heat transfer coefficients and with overall friction for operation at Notch 8 (full load) with standard air. The frictional losses were estimated on the basis of the Millington and Hartles correlation. The heat release correlation of Equation 1 was used; the values assumed for the adjustable constants were those predicted by Equation 2 for 21% oxygen content. After air flow and other available brake quantities were matched within 2% at notch 8, the ability of the simulation to predict performance at six other notch positions (without any further tuning) was explored. Measured data for the GE engine at the various notch positions included input parameters such as engine speed, mass of fuel injected, intake and exhaust temperature and pressure, and volumetric efficiency. Output parameters included brake power, brake-specific fuel consumption (bsfc), brake mean effective pressure (bmep), air mass flow, air/fuel ratio; and brake thermal efficiency.

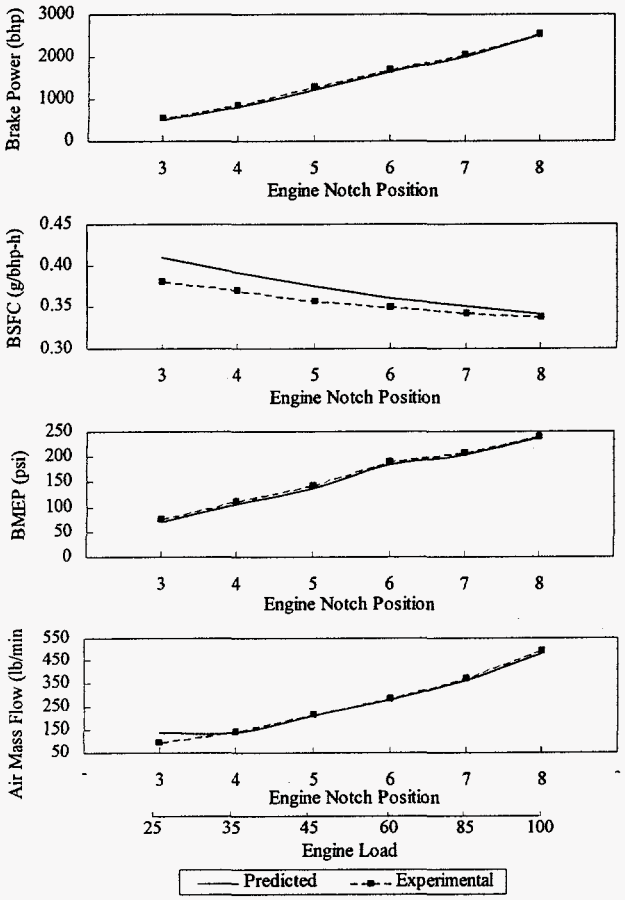

Fig. 3 Validation of DES model with experimental results

Figure 3 compares predicted brake power, bsfc, bmep, and air mass flow rate with corresponding measurements at all six notch positions. Over the range of notch positions examined, the diesel engine simulation under predicted brake power, bmep, and air flow by about 2% to 7%, while it correspondingly overpredicted bsfc by about 2% to 7%. Although agreement between baseline engine predictions and data could be improved by further tuning the model constants, it was felt that such an exercise was not warranted. First, a complete and reliable experimental database at all notch positions (specifically pressure and heat release rate) was not available when the diesel engine simulation was being matched to the engine. Further, the present study is intended to assess relative performance changes when the intake air for the engine is supplied with various oxygen levels, not to focus on baseline engine performance predictions.

Engine Gross Performance under Various Oxygen-Enrichment Levels

A constant oxygen-to-fuel ratio was used as the basis to compare engine performance under different levels of oxygen enrichment in the intake air. The mass of fuel injected per cylinder per cycle was increased proportionally to the oxygen level in the intake air to maintain a constant oxygen-to-fuel ratio. The gross brake power, bsfc, bmep, and peak cylinder pressure obtained when oxygen levels ranged from 21% to 35% (by volume) are shown in Figure 4 at all six notch positions. The amounts of power that would be required by the membrane to supply the desired intake air oxygen concentrations are not captured in the gross performance estimates but will be accounted for in a subsequent section to arrive at net performance improvements. The model predictions indicate that cylinder brake power significantly increases when the intake air oxygen concentration increases from 21% to 35%. A substantial (10%) output improvement can be achieved as the result of a relatively small increase in oxygen content to 23% by volume, while up to 90% improvements can be achieved when the oxygen content is increased to 35%. When the intake oxygen content was increased from 23% to 35%, the cylinder brake output increased from about 10% to 90% at notch positions 8 through 5. At lower notch positions (4 and 3), the cylinder output increased even more, by approximately 12% and 110% at oxygen-enrichment levels of 23% and 35%, respectively. The enhanced power output resulting from oxygen enrichment was accompanied by higher bmep and lower bsfc. At notch 8, the bsfc decreased from 0.339 to 0.29 g/bhp-h (about 15% reduction) when the intake air oxygen level was increased from 21% to 35%. A similar reduction in bsfc was observed at other notch positions, more predominantly at lower notch positions (4 and 3). The implied thermal efficiency improvements are attributed to faster burn rates, particularly during the diffusion phase of combustion (Assanis et al., 1990; Sekar et al., 1991a). Despite the advantages of lower bsfc, higher cylinder output, and higher bmep, the peak cylinder pressures were higher by about 3% to 35% when the intake air oxygen level was increased from 23% to 35%, respectively, over ambient air. However, the increase in peak cylinder pressure was smaller than the increase in cylinder output. This feature of the oxygen-enriched engine is attractive, particularly because some of the other techniques for increasing power output (increased compression ratio, high boost turbocharging) typically yield power improvements proportional to peak pressure increases.

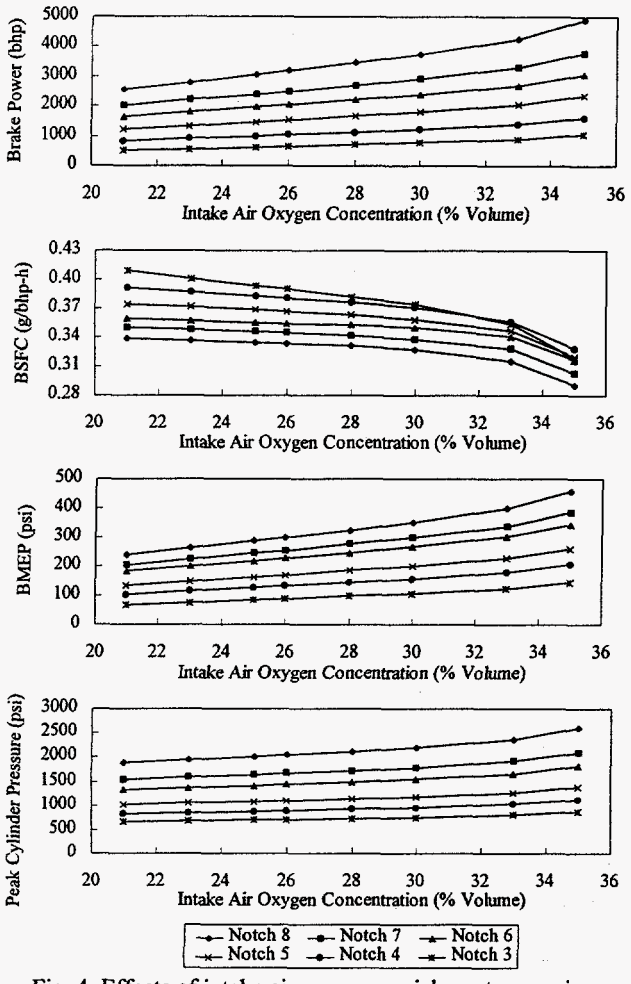

Fig. 4 Effects of intake air oxygen-enrichment on engine performance at various notch positions

Effects of Fuel Injection Timing with Oxygen-Enrichment

Oxygen-enriched combustion leads to shorter ignition delays, higher diffusion burn rates, and faster completion of the combustion process (Sekar et al., 1991a). These effects should permit the fuel injection timing to be retarded to contain the peak cylinder pressure within a specified ceiling while still allowing some of the performance benefits resulting from oxygen enrichment to be realized. Retarded fuel injection timing should also help to lower combustion temperatures and NO formation levels associated with oxygen enrichment.

Figure 5 shows the effects of fuel injection timing on the performance characteristics of an engine operating at full load (notch 8) with intake air at various oxygen-enrichment levels (23% to 30% by volume). As a result of retarding the fuel injection timing by four crank angle (CA) degrees, the deterioration in brake power, bsfc, and bmep was marginal (<1%) compared with the decrease in peak cylinder pressure (about 7%). Retarding the injection timing further (up to 12 CA degrees) combined with oxygen enrichment resulted in a reduction in the engine power output and bmep of about 4% and an increase in bsfc of about 4%. However, the corresponding peak cylinder pressure decreased by approximately 22% almost uniformly within the range of oxygen contents examined. The additional oxygen available in the combustion air shortened the ignition delay of the fuel-air mixture and thus the magnitude of the premixed heat release as captured by the heat release correlation. In addition, the faster diffusion burn rates still allowed combustion to proceed in an optimal manner, so it reached its peak within 16 CA degrees after TDC for the optimal retarding of timing. Figure 6 illustrates an injection timing map showing the relationship between brake power and peak cylinder pressure for various oxygen levels in the intake air. By retarding fuel injection timing between 4 and 8 CA degrees for the various oxygen-enrichment levels, the peak cylinder pressure can be brought down to that achieved when standard air is used. The corresponding decrease in brake power and increase in bsfc at any particular oxygen-enrichment level was only about 3%. For example, at a constant peak cylinder pressure (like that of the base engine), the cylinder brake output increased by about 45% when the intake air oxygen level was increased from 21% to 30%

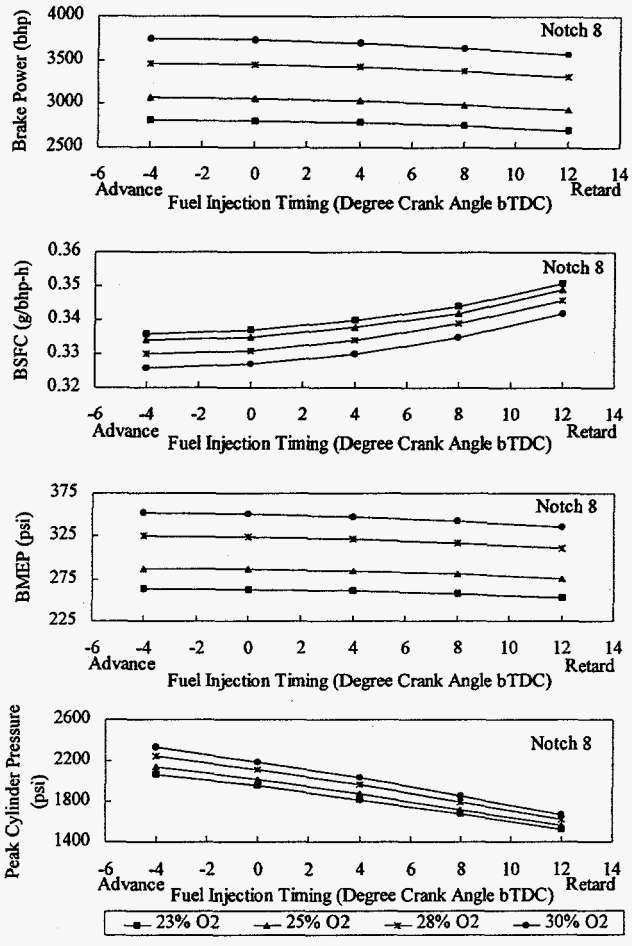

Fig. 5 Effects of fuel injection timing on performance characteristics at various oxygen-enrichment levels

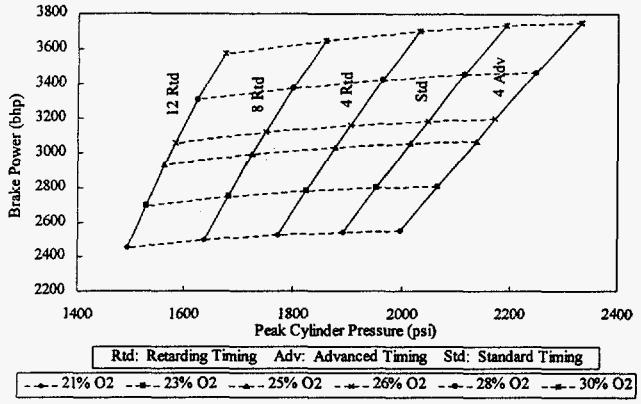

Fig. 6 Fuel injection timing map: Brake power versus peak cylinder pressure at various intake air oxygen-enrichment levels

and the fuel injection timing was retarded by about 8 CA degrees. The higher cylinder brake output at the same or a marginally higher peak cylinder pressure is clearly one advantage of oxygen-enriched combustion over other methods of increasing the power output from a given engine displacement.

NO Emissions

Higher post-flame temperatures and oxygen concentrations during the combustion process result in high NO formation rates (Heywood, 1988). For a given combustion chamber, NO emissions correlate with variations in the stoichiometric flame temperature, which is dependent on inlet pressure and temperature and the chemical composition of the fuel and oxidant (Plee et al., 1982). In the present work, variations in the stoichiometric, adiabatic flame temperature with changes in the oxygen concentration in the combustion air were studied by keeping all other influencing parameters (inlet pressure, temperature, and fuel composition) constant. The instantaneous traces of adiabatic flame temperature and overall, bulk gas temperature when 21% and 26% oxygen concentrations were used are depicted in Figure 7. When the intake oxygen concentration was increased from 21% to 26% (by volume), the peak stoichiometric flame temperatures and the gas temperatures were higher by about 240 K. This result can be readily explained, since the extra number of oxygen molecules in oxygen-enriched combustion displace nonreacting nitrogen molecules, which normally act as a diluent and cool down the flame. This result corroborates the correlation of adiabatic flame temperature with intake air effects, as established by several other researchers (Sawyer et al., 1973; Plee et al., 1982).

The NO formation histories during the combustion period are shown in Figure 8 for both ambient air and 26% oxygen-enriched intake air. Instantaneous NO concentrations are shown as a fraction of the contents in the burned core zone and the overall cylinder. The instantaneous NO concentrations were considerably higher with 26% oxygen-enriched intake air than with standard air. As combustion temperatures dropped, the NO concentrations froze at concentrations higher than equilibrium at the given temperature and pressure. The cycle-integrated, NO concentrations (as a fraction of the adiabatic burned gas and the

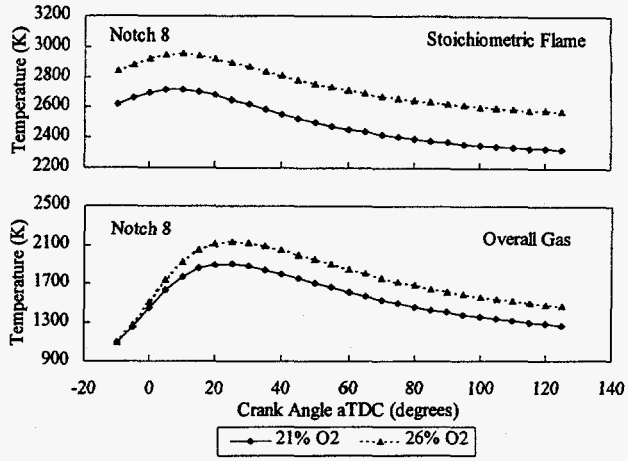

Fig. 7 Overall combustion and stoichiometric core-flame temperatures with intake air oxygen-enrichment

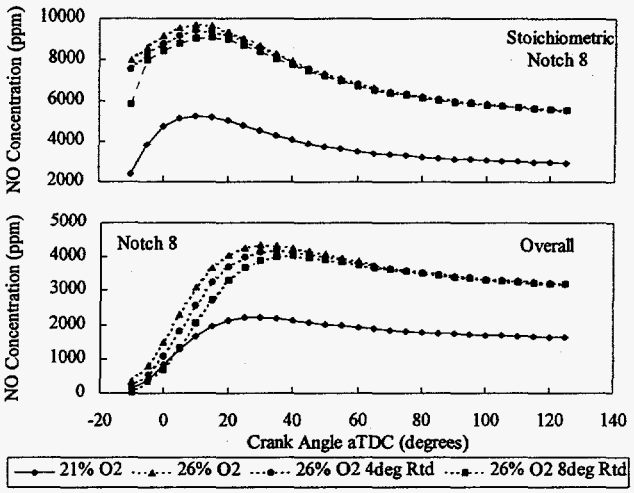

Fig. 8 Effects of oxygen and injection timing on NO emissions in stoichiometric and overall combustion regions

overall gas) are shown in Figure 9 for various oxygen-enrichment levels. Evidently, the NO emissions increased significantly when the intake air oxygen concentrations were increased. For instance, when the intake oxygen was increased from 21% to 26%, the cylinder-out NO emissions increased by about 2,100 parts per million (ppm). During operation at 30% oxygen content, the NO emissions increased by a factor of three, from 1,600 to 5,000 ppm. This increase in NO concentration corroborates previously published results on the effects of oxygen enrichment on NO emissions (Ghojel et al., 1983; Iida and Sato, 1988).

Higher NO emissions, which are concomitant with higher combustion temperatures are one of the major drawbacks of oxygen-enrichment technology. As a possible remedy, fuel injection timing was varied to examine whether it could influence the NO formation associated with oxygen enrichment. When the injection timing was retarded, the peak cylinder pressure and maximum overall in-cylinder gas temperatures decreased.

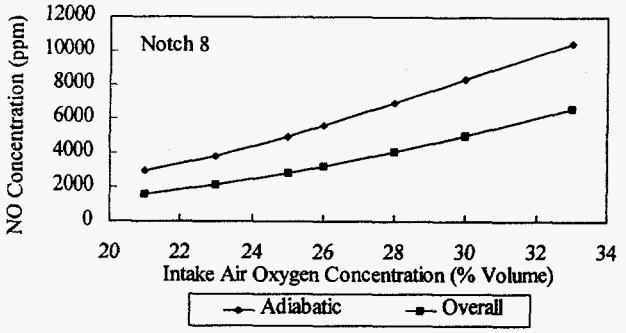

Fig. 9 Nitric oxide concentrations at different intake air oxygen-enrichment levels

However, computations showed that engine-out NO emissions decreased by only 50 to 100 ppm when fuel injection timing was retarded 4 to 12 CA degrees and oxygen-enriched intake air was used. However, the NO emission reductions obtained as a result of retarding fuel injection timing were marginal compared with the NO emission increases obtained when the oxygen concentration was increased from 21% to 26%. This result can be attributed to the fact that retarding injection timing does little to affect flame temperature, which is dominantly impacted by an increased oxygen concentration in the air. It appears that other control technologies are needed to overcome the NO penalty associated with oxygen enrichment. Some methods that have been explored to keep NO levels reasonably low when oxygen-enriched intake air is used include adding water in either the intake air or the fuel (Assanis et al., 1990) and using monatomic nitrogen induced by a pulsed arc, as a post-treatment device (Ng et al., 1995).

Membrane Size and Power Requirements

An estimation of the power required by the membrane to supply the desired level of oxygen-enrichment is necessary to assess the net power improvement obtained from an engine operating with oxygen-enriched intake air. The simplified membrane model was used to compute the membrane power and size reauired for an engine operating at full load and different intake air oxygen-enrichment levels. The predicted variation in permeate oxygen concentration with stage cut at various feed-to-permeate pressure ratios is shown in Figure 10 for CMS-3 membrane material. To yield high stage cut and high purity, both *selectivity and permeability should be high; these properties are* difficult to achieve because of the inherent tradeoffs between membrane permeability and selectivity. Data on the feed flow rate, permeate flow rate and pressure ratios across the module were used to obtain the membrane power data. The total isentropic work required to drive the membrane module to produce the desired oxygen concentration and the permeate flow rate under the three alternative operating modes are shown in Figure 11. The pressure mode is clearly the most power intensive because the pumping work is done on the feed air. On the other hand, the mixed mode requires the least power for moderate levels (up to 26%) of permeate oxygen. At higher permeate oxygen levels, the vacuum mode requires less power

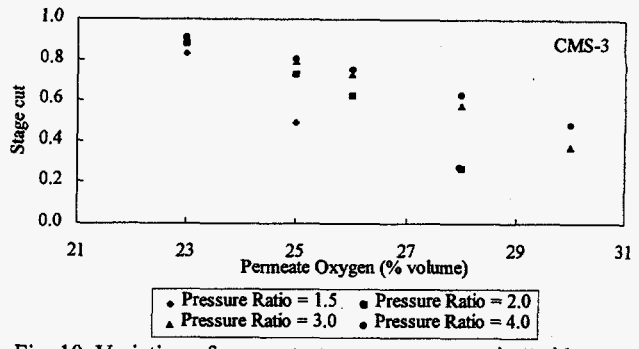

Fig. 10 Variation of permeate oxygen concentration with stage cut at various pressure ratios for CMS-3 membrane material

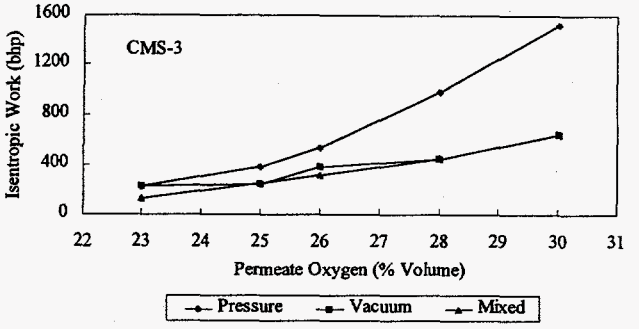

Fig. 11 Total isentropic work required to drive membrane under three operating modes

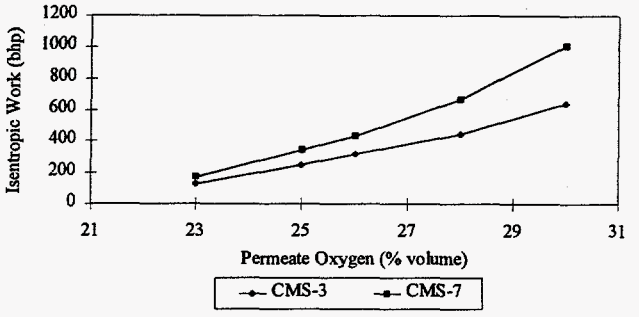

Fig. 12 Minimum isentropic work required by membrane module at various oxygen-enrichment levels

than the other two modes; mainly because the purity of the *oxygen concentration of the mixing stream is limited to 30%* or less (by volume) when either CMS-3 or CMS-7 membrane material is used. The minimum amount of isentropic work required to yield a prescribed level of permeate oxygen under full-load engine operation (Notch 8) is shown in Figure 12 for both CMS materials. CMS-3 requires less power because of its selectivity and stage cut are relatively hihger than those of CMS-7.

Table 3 compares some membrane performance parameters, including surface area, module volume, and isentropic work, required to supply 26% oxygen-enriched air to a locomotive engine operating at full load. The CMS-3 module occupied more space but required less power than the CMS-7 module.

Table 3. Design estimates of membrane size and power requirements for two different materials operating under mixed mode to supply 26% oxygen in the intake air of an engine at full load.

Material	Membrane surface area (10^3 square feet)	Active fiber length (feet)	No. of fibers (10^3)	Module volume (cubic feet)	Approximate cylindrical module dimensions (L x D) (feet)	Membrane isentropic work (bhp)
CMS-3	23.68	3	1,532	37	3 x 4	318
		4	1,150	28	4 x 3	
CMS-7	8.13	3	527	12.7	3 x 2.3	431
		4	395	9.5	4 x 1.7	

The tradeoff between membrane size and power is apparent. This tradeoff is inherent in membranes because of thier intrinsic properties (permeability versus selectivity). For example, CMS-3 has a relatively low permeability but high selectivity and thus requires less power but a larger module size. Conversely, CMS-7 has a relatively high permeability but low selectivity and thus required more power but a smaller module size. The tradeoffs among membrane properties and operating modes suggest that a detailed optimization study should be conducted to arrive at the smallest possible size and lowest amount of power required for any given application.

Performance of the Engine with Membrane Supplying Oxygen-Enriched Air

The work required by an air separator membrane to supply the desired oxygen concentration in the engine intake air has to be considered to evaluate the net brake output obtained from the engine. Computation of the parasitic power requirements of an air separator module involves optimizing several physical and operating characteristics of the membrane. Because design information is limited and there is no detailed membrane model, the accuracy of estimating membrane power requirements is compromised. However, for the preliminary membrane design arrived at in the previous section, membrane power requirements were estimated as a function of the permeate oxygen level for two candidate materials (Figure 12). Assuming that an air separator module made of CMS-3 membrane material and operating under the mixed mode supplies the desired oxygen concentration in the intake air, the net brake power output (cylinder brake power minus membrane work) was computed at full load, as shown in Figure 13. On the basis of the present membrane model, the net engine power improvements were found to be about 4% to 15% when the intake air oxygen was increased to 23% and 30%, respectively. Evidently, the net brake power improvements obtained from the engine that used oxygen-enriched intake air were considerably smaller than the gross cylinder output (without allowing for membrane work). Any reduction in membrane power requirements would directly enhance the net power improvements. However, for a detailed design and ultimate assessment of the membrane potential, more accurate computations of membrane power requirements should be carried out. They should consider all tradeoffs among membrane intrinsic properties and operating conditions.

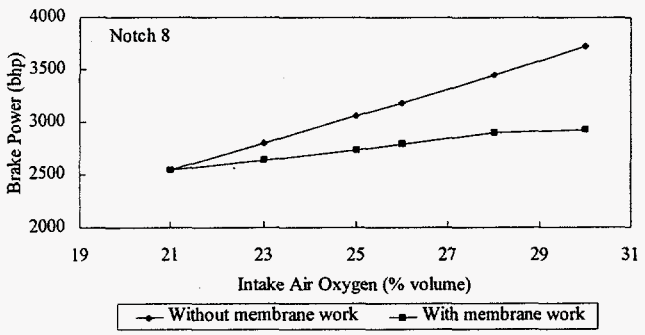

Fig. 13 Potential of brake power enhancement with oxygen-enrichment at full load

Oxygen Enrichment versus Turbocharging

Turbocharging is a proven, practical method to obtain a higher power output than the natural aspiration from a given engine displacement. However, there are practical limits to boosting intake manifold pressure before the complexity and losses associated with compressing the air are increased considerably (e.g., need for two-stage turbocharging and intercooling). Use of oxygen-enriched intake air can be considered as an alternative or a complementary method to boost the power output. In the present work, an attempt was made to quantify the difference between highly boosted turbocharging versus oxygen enrichment plus regular boost, in terms of the brake power obtainable at any specified peak cylinder pressure.

To admit the same mass of oxygen per cycle as that which occurs with oxygen enrichment, turbocharging requires a considerably higher intake manifold pressure. At full load, turbocharging requires the intake manifold pressure to be increased from 35 to 57 psi to deliver the mass of oxygen equivalent to 21% to 35% oxygen enrichment levels, respectively. The same mass of fuel is injected in both cases, so that they operate with the same oxygen-to-fuel ratio. The considerably increased compression work resulting from the highly boosted air and its extra mass of nitrogen are reduced in the case of oxygen enrichment. As a result, the gross cylinder power obtained is considerably higher with oxygen enrichment than with high-boost turbocharging at any constant peak cylinder pressure (see Figure 14). When the membrane power is subtracted from the cylinder output, the difference between oxygen enrichment and turbocharging appears to be minimal for operation at the base injection timing (Figure 14). However, an oxygen-enriched engine, with its shorter delay and faster diffusion burn period, can afford injection timing that is retarded so that peak cylinder pressure is reduced, as discussed previously. When this strategy is followed, the net brake power obtainable at any constant peak cylinder pressure is higher with oxygen

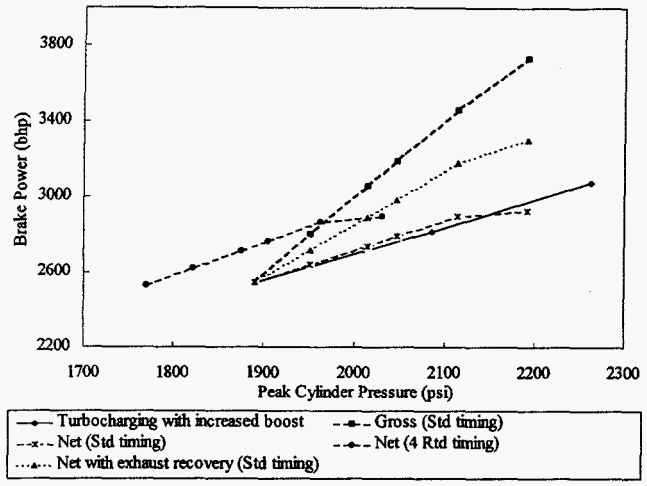

Fig. 14 Potential of oxygen-enrichment over turbocharging with increased boost to enhance the power output

enrichment than with high-boost turbocharging. For instance, by using 28% oxygen concentration and fuel injection timing retarded by 4 CA degrees, a 4% increase in peak cylinder pressure could result in an increase in engine net power of approximately 13%, compared with an increase of only 4% by using turbocharging. In general, power enhancement with increased turbocharging is fairly proportional to the increase in peak cylinder pressure, whereas the benefit is almost doubled with oxygen enrichment.

At a constant oxygen-to-fuel ratio, exhaust gas temperatures at the turbine exit were considerably higher (100 to 500 K) with oxygen enrichment than with turbocharging because of the higher flame temperatures of the former. If part of the additional exhaust energy what is available with oxygen enrichment were recovered, the net power improvement of the oxygen-enriched engine would be more attractive. To quantify the expected improvement, the difference in exhaust enthalpy past the turbine under operation with oxygen enrichment versus increased inlet boost was assumed to be recovered by using an organic rankine cycle with 20% overall thermal efficiency. The additional power obtained from the recovered exhaust energy was then added to the net brake power of the oxygen-enriched engine, as shown in Figure 14. For a 12% increase in peak cylinder pressure, the net power obtained by using oxygen-enriched air with exhaust recovery increased from 14% to 25%, whereas the power improvement that resulted from using an increased inlet boost was only 13%. Hence, it is essential to recover part of the incremental exhaust energy with oxygen enrichment so that the net power improvements from a given engine are competitive with other conventional methods.

SUMMARY AND CONCLUSIONS

A thermodynamic diesel engine simulation and a simplified model of the air separator membrane were used to study the effects of different intake air oxygen-enrichment levels on the performance and NO emissions of a locomotive diesel engine. The following conclusions can be drawn from this investigation:

1. At notch 8 (full load), when the intake air oxygen concentration was increased from 21% to 35% (by volume) while a constant oxygen-to-fuel ratio was maintained in the combustion mixture, the cylinder brake output and brake mean effective pressure increased by up to 90%, and brake-specific fuel consumption decreased by down to 15%. However, the corresponding peak cylinder pressure increased by up to 35%.
2. Retarding the fuel injection timing when oxygen-enriched intake air is used has a beneficial effect with respect to peak cylinder pressure without imposing a severe penalty on power and fuel consumption. When various intake air oxygen levels between 23% and 30% (by volume) and retarded fuel injection timing (up to 12 degrees crank angle) were used, the peak cylinder pressure decreased by up to 22%, and only a marginal penalty (on the order of 4%) in power and fuel consumption resulted.
3. NO emissions computed on the basis of adiabatic flame temperature increased by up to 4 times when the intake air oxygen concentration was increased from 21% to 35%. Although retarding fuel injection timing can somewhat reduce NO emissions associated with oxygen-enriched combustion, another post-treatment device is needed to comply with the NO emission standards.
4. To provide intake air with 23% to 30% oxygen content (by volume) for a 12-cylinder locomotive diesel engine operating at full load requires between 150 to 800 bhp to drive the auxiliary equipment; the corresponding membrane area is estimated to occupy between 10 and 30 cubic feet, depending on the desired level of oxygen enrichment. However, an extensive optimization of several membrane parameters is necessary to refine the estimates of membrane power and size for a desired enrichment level and air flow.
5. On the basis of a preliminary membrane design and its power requirements, the net brake power improvement obtained from an engine operating with oxygen-enriched air (from 23% to 30% by volume) supplied by an air separation membrane was only between 4% and 15%. For the same inlet conditions, the cylinder brake output (without the parasitic membrane work) improved substantially, i.e. between 10% and 46%. Any reduction in membrane power requirements has an obvious direct impact on net power improvement.
6. When peak cylinder pressure is controlled by retarding fuel injection timing, oxygen enrichment has the potential to result in greater improvements in brake power than those obtained by using other methods such as high-boost turbocharging. For instance, a 4% increase in peak cylinder pressure can result in a 13% increase in net engine power with oxygen enrichment but only a 4% increase with high-boost turbocharging. In addition, recovering part of the increased exhaust energy through a bottoming cycle can make the oxygen-enriched concept far more attractive than other methods of boosting power at a constant peak cylinder pressure.

7. Since the required modifications to the intake system are not complex, a membrane device can be readily retrofitted to in-use locomotives. Oxygen-enrichment technology promises to provide a significant power boost on sudden demand or continuously, alleviate concerns about certain exhaust emissions (visible smoke, particulates, and unburned hydrocarbons), and enable the use of lower grade fuels.

ACKNOWLEDGMENTS

The authors acknowledge the support of the U.S. Department of Energy, Office of Energy Research, under contract W-31-109-Eng-38. The contributions of V.O. Markworth, Southwest Research Institute, in supplying experimental data are greatly appreciated. The authors thank Stuart Nemser, Compact Membrane Systems, Inc., for providing details on membrane properties and design. The contributions of Dr. Zoran Filipi in simulating the baseline locomotive engine are gratefully acknowledged. Assistance from Anthony Markel and Kevin Stork while the manuscript was being prepared is very much appreciated.

REFERENCES

Assanis, D.N., and J.B. Heywood, *Development and Use of a Computer Simulation of the Turbocompound Diesel Engine System for Engine Performance and Component Heat Transfer Studies*, SAE Paper 860329, 1986.

Assanis, D.N., R.R. Sekar, D. Baker, C.T. Ciambekos, R.L. Cole, and T.J. Marciniak, *Simulation Studies of Diesel Engine Performance with Oxygen Enriched Air and Water Emulsified Fuels*, ASME Paper 90-ICE-17, 1990.

Assanis, D.N., E. Karvounis, R.R. Sekar, and W.W. Marr, *Heat Release Analysis of Oxygen-Enriched Diesel Combustion*, ASME Journal of Engineering for Gas Turbine and Power, Vol. 115, pp. 761-768, 1993.

Chern, R.T., W.J. Koros, and P.S. Fedklw, *Simulation of a Hollow-Fiber Gas Separator: The Effects of Process and Design Variables*, Ind. Eng. Chem. Process Des. Dev., Vol. 24, pp. 1015-1022, 1985.

Ghojel, J., J.C. Hillard, and J.A. Levendis, *Effect of Oxygen-Enrichment on the Performance and Emissions of IDI Diesel Engines*, SAE Paper 830245, 1983.

Gollan, A.Z., and M.H. Kleper, *Research into an Asymmetric Membrane Hollow Fiber Device for Oxygen-Enriched Air Production*, DOE/ID-12429-1, U.S. Department of Energy, 1985.

Heywood, J.B., *Internal Combustion Engine Fundamentals*, McGraw-Hill Book Company., 1988.

Iida, N., and G.T. Sato, *Temperature and Mixing Effects on NO_x and Particulates*, SAE Paper 880424, 1988.

Koros, W.J., and R.T. Chern, *Handbook of Separation Process Technology*, John Wiley and Sons, 1987.

Lavoie, G.A., J.B. Heywood, and J.C. Keck, *Experimental and Theoretical Investigation of Nitric Oxide Formation in Internal Combustion Engines*, Combustion Science and Technology, Vol. 1, pp. 313-326, 1970.

Markworth, V.O., S.K. Widener, A.C. Matheaus, and R.L. Mason, *Locomotive Improvement Program - Twelfth Research Phase Final Report*, SwRI Report No. 03-4171/AAR Report No. R-841, 1993.

Marr, W.W., R.R. Sekar, R.L. Cole, T.J. Marciniak, and D.E. Longman, *Oxygen-Enriched Diesel Engine Experiments with a Low-Grade Fuel*, SAE Paper 932805, 1993.

Ng, H.K., V.J. Novick, and R.R. Sekar, *Using Monatomic Nitrogen Induced by a Pulsed Arc to Remove Nitrogen Oxides from a Gas Stream*, ASME Fall Technical Conference, Vol. 1, pp. 73-80, 1995.

Nemser, S.M., and I.C. Roman, *Perfluorodioxole Membranes*, U.S. Patent 5,051,114, 1991.

Pan, C.Y., *Gas Separation by High-Flux, Asymmetric Hollow-Fiber Membrane*, AIChE Journal, Vol. 32, No. 12, pp. 2020-2027, 1986.

Plee, S.L., T. Ahmad, and J.P. Myers, *Diesel NO_x Emissions - A Simple Correlation Technique for Intake Air Effects*, Nineteenth Symposium (International) on Combustion, The Combustion Institute, pp. 1495-1502, 1982.

Ragland, K.W., and J.G. Whipple, *Test and Evaluation of Polymeric Membranes for Oxygen-Enrichment of Air*, DOE/ID-12710-1, U.S. Department of Energy, 1989.

Sawyer, R.F., N.P. Cernansky, and A.K. Oppenheim, *Factors Controlling Pollutant Emissions from Gas Turbine Engines*, Atmospheric Pollution by Aircraft Engines, AGARD CP-125, Paper No. 22, 1973.

Sekar, R.R., W.W. Marr, R.L. Cole, T.J. Marciniak, and J.E. Schaus, *Diesel Engine Experiments with Oxygen Enrichment, Water Addition, and Lower-Grade Fuel*, Twenty-Fifth Intersociety Energy Conversion Engineering Conference, Reno, Nevada, 1990.

Sekar, R.R., W.W. Marr, D.N. Assanis, R.L. Cole, T.J. Marciniak, and J.E. Schaus, *Oxygen-Enriched Diesel Engine Performance: A Comparison of Analytical and Experimental Results*, ASME Journal of Engineering for Gas Turbine and Power, Vol. 113, pp. 365-369, 1991a.

Sekar, R.R., W.W. Marr, R.L. Cole, and T.J. Marciniak, *Effects of Oxygen Enrichment and Fuel Emulsification on Diesel Engine Performance and Emissions*, ASME Meeting on Fuels, Controls and After-treatment for Low-Emissions Engines, ICE., Vol. 15, pp. 21-28, 1991b.

Winston Ho, W.S., and K.K. Sirkar, *Membrane Handbook*, Chapman & Hall, N.Y., 1992.